



Technical Note

New type of $[\text{Bi}_6\text{O}_6(\text{OH})_3](\text{NO}_3)_3 \cdot 1.5\text{H}_2\text{O}$ sheets photocatalyst with high photocatalytic activity on degradation of phenol



Yuxiao Yang^{a,1}, Huoyan Liang^{a,1}, Na Zhu^{a,1}, Yaping Zhao^{c,*}, Changsheng Guo^{b,*}, Lu Liu^{a,*}

^a College of Environmental Science and Engineering, Nankai University, Tianjin 300071, China

^b Department of Environmental Science, East China Normal University, Shanghai 200062, China

^c State Key Laboratory of Environmental Criteria and Risk Assessment, Chinese Research Academy of Environmental Sciences, Beijing 100012, China

HIGHLIGHTS

- Novel $[\text{Bi}_6\text{O}_6(\text{OH})_3](\text{NO}_3)_3 \cdot 1.5\text{H}_2\text{O}$ sheets photocatalyst was synthesized and characterized.
- The catalyst exhibited better photocatalytic effects superior to that of classic TiO_2 P25.
- Photodegradation mechanism was direct oxidation/reduction product of phenol by $\text{HO}^\bullet/\text{O}_2^-$.

ARTICLE INFO

Article history:

Received 25 March 2013

Received in revised form 19 June 2013

Accepted 20 June 2013

Available online 14 August 2013

Keywords:

$[\text{Bi}_6\text{O}_6(\text{OH})_3](\text{NO}_3)_3 \cdot 1.5\text{H}_2\text{O}$

Phenol

UV illumination

Photocatalysis

ABSTRACT

A new type of $[\text{Bi}_6\text{O}_6(\text{OH})_3](\text{NO}_3)_3 \cdot 1.5\text{H}_2\text{O}$ sheets photocatalyst was synthesized via a hydrothermal route. The photocatalytic properties were characterized by SEM, TEM, XRD and UV spectroscopy. It exhibited slightly better photocatalytic activity on phenol degradation than that of classic TiO_2 P25 under UV illumination. Hydroquinone, catechol, resorcinol, and benzoquinone were identified as photodegradation intermediates. It has the advantages of high effective photodegradation efficiency and easy separation properties.

Crown Copyright © 2013 Published by Elsevier Ltd. All rights reserved.

1. Introduction

Various contaminants such as azo dyes, organochlorine and aromatic hydrocarbons in natural water environments have been detected. At present, some promising technologies such as biological methods (Fukuda et al., 2001; Kang and Kondo, 2002; Xuan et al., 2002; Fent et al., 2003) have been used for eliminating organic pollutants. Highly effective treatment methods are necessary for transforming organic pollutants into CO_2 and water. Owing to mineralization of organic substances, advanced oxidation processes (AOPs) have drawn great attention during the last two decades. AOPs have been studied to alleviate the deterioration of natural environments created by toxic pollutants. In AOPs, the metal oxide TiO_2 , is often used as a catalyst. For example, TiO_2 nanoparticles (Kong et al., 2011; Tachikawa et al., 2011), nanotubes (NTs) (Macak et al., 2007), nanobelts (Zhou et al., 2011), nanosheets (Yang et al., 2009) and mesosponge layers (Lee et al., 2010), have been explored

for photocatalytic applications. The unique photocatalytic properties of TiO_2 have attracted increasing interest (Fujishima et al., 2008).

Very recently, 3D ordered TiO_2 assemblies of NTs have arisen great attention (Zheng et al., 2009; Liu et al., 2010), and a few materials have been synthesized and applied in mineralization of endocrine disrupting chemicals (Liu et al., 2008; Guo et al., 2010). The advantages of the microspheres are: (1) there are high surface-to-volume ratios with effective prevention of further aggregation of the nanoparticles, so as to retain high catalytic activity and (2) due to the energy difference between the lowest unoccupied and highest occupied molecular orbitals, size-quantized, nanometer-sized semiconductor particles have higher redox potentials as a result of the increase in band-gap energy (Liu et al., 2008). Although 3D microsphere catalysts have been improved, it is still difficult for both nanomaterials and water to be separated after water treatment. Therefore synthesis of new catalysts is necessary to achieve highly effective photodegradation and easier separation.

In the present paper, a facile hydrothermal method was applied to synthesize a new type of photocatalyst, bulk $[\text{Bi}_6\text{O}_6(\text{OH})_3]$

* Corresponding authors. Tel.: +86 20 23504849 (L. Liu).

E-mail addresses: ypzhao@des.ecnu.edu.cn (Y. Zhao), guocs@cras.org.cn (C. Guo), liul@nankai.edu.cn (L. Liu).

¹ Tel.: +86 20 23504849.

(NO₃)₃·1.5H₂O sheets, which comprised tooth meshing side faces. The preparation method is simple and mild, and no templates were used during the whole synthetic route. The catalyst was used for the photocatalytic degradation of phenol, a typical organic compound. The degradability and degradation kinetics including the reaction products were identified by HPLC–MS analysis. The degradation intermediates/products were further applied to investigate the reaction pathways.

2. Materials and methods

2.1. Materials

All chemicals were of analytical grade and used as received without further purification. The [Bi₆O₆(OH)₃](NO₃)₃·1.5H₂O catalysts were synthesized via a hydrothermal process. In a typical preparation of the [Bi₆O₆(OH)₃](NO₃)₃·1.5H₂O sample, 0.485 g of Bi(NO₃)₃·5H₂O was dissolved in 20 mL of distilled water, and the resulting solution was stirred for 20 min. Afterward, all was transferred to a 30 mL Teflon-lined autoclave, which was filled with water to 80% of its total volume. The autoclave was then heated at 180 °C for 12 h, and it was allowed to cool to room temperature. The product in the autoclave was collected, washed with deionized water and absolute ethanol, and dried at 80 °C for 2 h. The dried samples were then stored for further use (sample A). To study the influence of reactant concentration on morphologies, 0.2 and 0.4 g Bi(NO₃)₃·5H₂O were respectively added into the system while keeping other conditions unchanged. The obtained products were denoted as sample B and sample C.

2.2. Sample characterization

XRD analysis was carried out using an X-ray diffractometer (Model D/MAX2500, Rigaku) with Cu K α radiation ($\lambda = 1.54056$ Å). The morphology of the as-prepared products was characterized by scanning electron microscopy (SEM, Hitachi-530, SEM/EDX JEOL JSM-6700F) and transmission electron microscopy (TEM, JEOL-2010, operating voltage of 200 kV). The UV–Vis diffuse reflectance spectra (DRS) were measured by Shimadzu UV-3600 UV–Vis spectrophotometer.

2.3. Photocatalytic activity evaluation

The photocatalytic activity of the samples was monitored through the degradation of phenol under UV (300 W Hg lamp) in a cylindrical quartz reactor with water circulation facility. 0.2 g photocatalyst and 200 mL phenol solution with the initial concentration of 10 mg L⁻¹ were added into the reactor and stirred in dark for 30 min to achieve adsorption–desorption equilibrium. The pHs of reaction solutions without adjusting pH were 5.74 and reaction was performing at 20 ± 1 °C. The parallel experiments were done with the RSD less than 5%. Then the light was turned on, and about 3 mL aliquot of the reaction solution was taken at time interval of 15 min during the experiment. The solution was filtrated through 0.45 μ m water filter, and the concentration of phenol was evaluated at the wavelength of 270 nm with a UV–Vis spectrophotometer (UV2550, Shimadzu). Total organic carbon (TOC) was measured on a Shimadzu TOC-V CPH analyzer.

The intermediates formed during the photocatalytic process were monitored by HPLC/MS (Agilent 6410 triple quadrupole) equipped with an electrospray ionization source (ESI) in negative ionization mode. MS spectra were acquired using a selective ion monitoring mode with a dwell time of 200 ms and the scan range m/z was detected from 50 to 300. The HPLC separation was performed using an Agilent 1200 series (Palo Alto, CA, USA) equipped with an Agilent Zorbax Eclipse XDB-C18 column (2.1 × 100 mm, 3.5 μ m). During the sample analysis, the column was maintained at 30 °C. The intermediates were detected in an isocratic elution program. Methanol/water = 40:60 (v/v) were used as mobile phase, the injection volume was 10 μ L, and flow rate was set at 0.2 mL min⁻¹.

3. Results and discussion

3.1. Properties of the catalyst

XRD was used to characterize the phase structure of the obtained products. It can be seen from Fig. 1a that the XRD pattern is in conformity with tetragonal [Bi₆O₆(OH)₃](NO₃)₃·1.5H₂O ($a = b = 3.818$ Å, $c = 17.149$ Å, JCPDS: 53-1038). No characteristic peak was observed for other impurities such as Bi₂O₃, Bi(NO₃)₃, and Bi, which indicates that pure crystalline [Bi₆O₆(OH)₃](NO₃)₃·1.5H₂O was formed via the hydrothermal process. In Fig. 1a, it

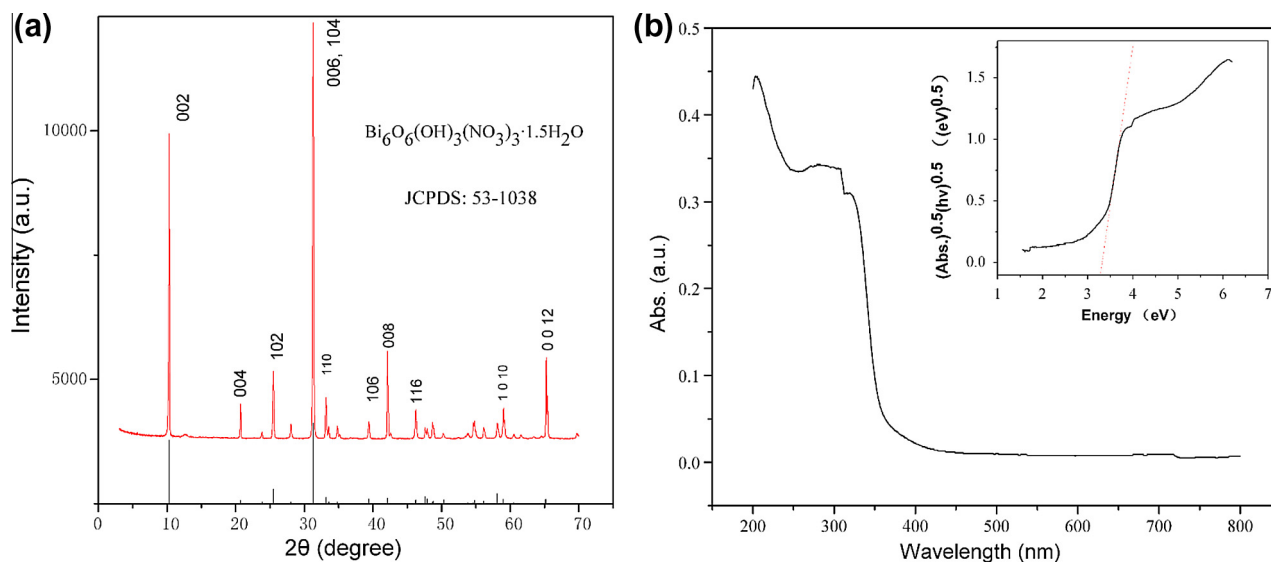


Fig. 1. XRD (a) and UV–Vis DRS (b) of the sample (inset: plots of $(\alpha h\nu)^{1/2}$ vs photon energy ($h\nu$)).

Download English Version:

<https://daneshyari.com/en/article/4409231>

Download Persian Version:

<https://daneshyari.com/article/4409231>

[Daneshyari.com](https://daneshyari.com)